

# The Jamming Transition in Granular Systems – Supplementary Information

T. S. Majmudar<sup>1</sup>, M. Sperl<sup>1</sup>, S. Luding<sup>2</sup>, R.P. Behringer<sup>1</sup>

<sup>1</sup>Duke University, Department of Physics, Box 90305, Durham, NC 27708, USA,

<sup>2</sup>Technische Universiteit Delft, DelftChemTech, Particle Technology, Nanostructured Materials,

Julianlaan 136, 2628 BL Delft, The Netherlands

(Dated: February 2, 2007)

## I. SUPPLEMENTARY METHODS

In this supplement, we provide experimental details which we discuss in the context of Fig. 1. A key point concerning the experiments is the use of photoelasticity (stress-induced birefringence) to obtain vector forces at interparticle contacts. This technique has the added advantage of determining to good accuracy whether a contact is present or not.

### a. Photoelastic Method and Determination of Contacts

A stressed photoelastic particle (in our case, a disk) when viewed through crossed circular polarizers, shows a pattern of light and dark bands. The light rays traversing the polarizers and a particle (along the axial direction of the disk) have an intensity  $I = I_0 \sin^2[(\sigma_1 - \sigma_2)C]$ . Here, the  $\sigma_i$  are the principle stresses within the particle;  $C$  is a constant that depends on the thickness and properties of the disk, and on the wavelength of the light [1]. Given a set of contacts for a disk, and forces at these contacts, the specific photoelastic pattern is determined. Here, we take advantage of the fact that a two-dimensional description for the stresses is appropriate. Assuming that the contact forces are well-approximated as point-like, the Boussinesq solution gives the stresses within the disk [2]. For these experiments, we solve the inverse problem: we have the light intensities of the photoelastic pattern within a disk, and we find the contact forces. We use an automated computer algorithm which uses the vector contact forces as nonlinear least-squares fit parameters. The fitting procedure minimizes differences between the experimentally measured intensity pattern for a disk and the intensity pattern that would be obtained for a given set of contact forces [3].

In order to improve the discrimination between false and true contacts we employ a two step process. The first step involves obtaining possible contacts based on the distances between disk centers; if the particle centers are within  $D \pm 0.1D$ , where  $D$  is the mean center-to-center distance of a particle pair, the disks are considered to be in potential contact. This estimate of contacts is markedly improved by utilizing the photoelastic stress images at various exposure times for each state, such that eventually most of the force transmitting contacts can be seen. As seen in Fig. 1b, the contacts through which there is force transmission, appear as source points for the stress pattern. This effect can be quantified by measuring the intensity and the gradient square of the intensity ( $G^2 = |\nabla I|^2$  where the gradient is taken in the plane of the disk) around the contact [4]. A true, force bearing contact can be distinguished by employing appropriate thresholds in intensity and in  $G^2$ . The thresholds in intensity and in  $G^2$  are useful in capturing contacts with very small forces, since these quantities are higher near force bearing contacts. The final er-

ror in average  $Z$  is around 3.5% for rather low  $\phi$ , and around 1.5% for higher  $\phi$ .

b. *Calibration of the Force Law* A direct mechanical calibration for the particles using a digital force gage is shown in Fig. S1: The dotted curve shows a force law  $F \propto \delta^{3/2}$ . A linear fit describes the calibration data well for  $\delta > 250\mu\text{m}$  which is comparable to the surface roughness of the cylinders. The photoelastic response is detectable for displacements that exceed the right end of the gray bar at  $\delta \approx 150\mu\text{m}$ . In the effective range for the photoelastic technique,  $\delta > 150\mu\text{m}$ , the force vs. displacement curve is reasonably well described by a straight line.

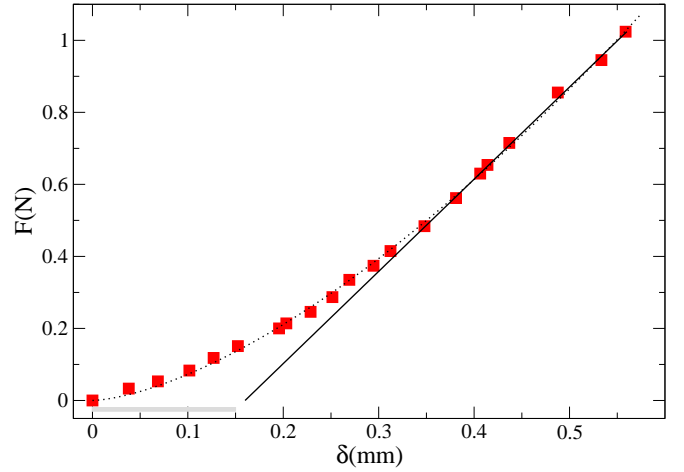


FIG. S1: Calibration of the contact force  $F$  for a representative disk pushed against a hard surface by a displacement  $\delta$ . The experimental data (squares) are fitted by the power law  $F = 2.52\text{N} (\delta^{1.54})$  (dotted) and by the linear law  $F = 2.56\text{N} (\delta - 0.16)$  (full curve). Here, all lengths are given in mm. The gray bar indicates the roughness of the cylinder surface. Photoelastic response is reliably detectable to the right of this bar.

## II. SUPPLEMENTARY TABLE

c. *Details of the Fitting Procedure* For the fit of the data with the power law  $Z - Z_c = a(\phi - \phi_c)^\beta$  we examine a range of values for  $\phi_c$  and obtain the exponents for the power-law fits given in Table SI. Here,  $\phi_c$  is selected, and  $Z_c$ , and  $\beta$  are the fitting parameters. For the case without rattlers,  $\beta$  ranges from 0.49 to 0.56, and  $Z_c$  ranges from 2.40 to 3.08. For the case with rattlers,  $\beta$  shows more variation (0.36 - 0.52), and the errors in  $Z_c$  are larger. For the entire range of  $\phi$ , the root

$\phi_c$	Without Rattlers			With Rattlers		
	$Z_c$	$\beta$	RMSE	$Z_c$	$\beta$	RMSE
0.84058	$2.397 \pm 0.135$	$0.517 \pm 0.064$	0.049	$1.198 \pm 0.310$	$0.502 \pm 0.093$	0.109
0.84075	$2.512 \pm 0.138$	$0.547 \pm 0.073$	0.051	$1.071 \pm 0.359$	$0.460 \pm 0.090$	0.103
0.84172	$2.632 \pm 0.151$	$0.494 \pm 0.077$	0.045	$0.9747 \pm 0.458$	$0.363 \pm 0.083$	0.080
0.84204	$2.858 \pm 0.127$	$0.564 \pm 0.086$	0.045	$1.183 \pm 0.413$	$0.367 \pm 0.079$	0.072
0.84220	$2.838 \pm 0.171$	$0.533 \pm 0.102$	0.046	$1.490 \pm 0.427$	$0.405 \pm 0.096$	0.072
0.84236	$2.916 \pm 0.133$	$0.556 \pm 0.093$	0.046	$1.744 \pm 0.298$	$0.445 \pm 0.088$	0.075
0.84269	$3.003 \pm 0.124$	$0.563 \pm 0.095$	0.043	$1.989 \pm 0.267$	$0.469 \pm 0.092$	0.071
0.84301	$3.075 \pm 0.120$	$0.560 \pm 0.095$	0.041	$2.280 \pm 0.235$	$0.525 \pm 0.108$	0.072

TABLE SI: Power-law exponents and critical contact numbers obtained as fitting parameters, at various critical packing fractions. The RMSE gives the root mean squared errors for the fits. The indicated uncertainties in both  $Z_c$ , and  $\beta$  are obtained from the 95% confidence interval of the best-fit parameter values.

mean squared errors (RMSE) are larger for the case with rattlers (0.071 - 0.109), than for the case without rattlers (0.041

- 0.051), indicating that power-law fits are consistently better when rattlers are excluded.

- 
- [1] M. Frocht, *Photoelasticity, Vol. I* (John Wiley & Sons, New York, 1941).  
[2] M. Frocht, *Photoelasticity, Vol. II* (John Wiley & Sons, New York, 1948).

- [3] T. S. Majmudar and R. P. Behringer, *Nature* **435**, 1079 (2005).  
[4] D. Howell, R. P. Behringer, and C. Veje, *Phys. Rev. Lett.* **82**, 5241 (1999).